




Algorithm for Selecting a Concrete Pump in the Construction of High-Rise Buildings

Velikanov, Nikolay Leonidovich^{1*} 

Naumov, Vladimir Arkad'evich² 

¹ Immanuel Kant Baltic Federal University, Kaliningrad, Russian Federation

² Kaliningrad State Technical University, Kaliningrad, Russian Federation

Correspondence:* email NVelikanov@kantiana.ru; contact phone [+7 4012595 595](tel:+74012595595)

Keywords:

Stationary piston concrete pump; Mixture transportation; Rheological model; Pressure loss

Abstract:

The use of concrete pumps allows you to mechanize and automate the main processes of laying concrete in construction, use additive technologies. To choose the right pump, you need to know the hydraulic characteristics of the network, the rheological properties of the mixture. **This article is devoted** to developing an algorithm for calculating the pump characteristics for specific construction conditions. **Method.** The algorithm is based on the empirical dependencies previously proposed by the authors for pump characteristics, mixture rheology, and hydraulic network characteristics. **Results.** For stationary piston concrete pumps, an example of calculations using the proposed algorithm is given. It is shown that when choosing a piston pump, information is needed about the value of the filling factor, the dependence of the total efficiency of the pump (or the power consumed) on the pressure drop.

1 Introduction

The use of concrete pumps in construction allows you to reduce manual labor and use additive technologies significantly. But this imposes several requirements on the rheological properties of cement materials. 3D printing using cement materials is an emerging technology and represents an active area of research. Rheological studies are important for successful 3D printing of concrete. The main task for successful 3D printing is the good characteristics of concrete. It must be sufficiently fluid to be pumped through the hose and gain sufficient strength and rigidity to build up after layer-by-layer deposition [1]. Despite this, only limited studies of the pumping behavior of fluids with high yield strength, such as printed concrete. The paper [2] presents the results of a study of the rheological behavior of cement materials for 3D printing with a different ratio of aggregate to a binder. An increase in this ratio leads to a significant increase in the plastic viscosity and a nominal increase in the yield strength.

To facilitate the study of the rheological properties of cement materials, researchers [3] modified a commercial bench-mounted three-dimensional printer for the production of fused filaments (3-D) for dosing cement paste mixtures. The changes included the design and assembly of the pumping system and the modification of the 3-D printer firmware software necessary to accommodate the new equipment.

In the study [4], a slag-based mixture was developed as a cementless material for stable spray 3D printing. To obtain the optimal mixture, the effect of the addition of MgO and fly ash to the cenosphere on the setting, hydration, and rheological properties of fresh mixtures were studied. The material with adapted rheology results in better feed and deposition performance of the mixture and improved spray printing quality.

In [5], the influence of a viscosity-modifying additive based on hydroxypropylmethylcellulose on 3D printing and mechanical characteristics of a cement material based on limestone and calcined clay was studied.

In the study [6], the rheological behavior of cement pastes with nanotubes and various types of polymer plasticizing impurities was analyzed using a rotating rheometer with coaxial cylinders.

The rheological properties of the lubricating layer between the bulk concrete and the pump pipe wall are a key factor determining the pumpability of concrete [7, 8]. In the study [9], the rheological behavior of the lubricating layer was modeled in the form of a suspension of different volume content of fine sand (<1.25 mm) in viscoelastoplastic cement pastes, namely, fine solutions.

The results obtained showed that an increase in the content of fine sand increases the relative viscoelastic properties of the studied mixtures. Several studies on the quantitative prediction of concrete pumping using the rheological properties of concrete and the lubricating layer have been conducted [10]. It was found that the pressure loss in the bends of the pipes is about twice large as in the straight pipeline.

It is shown [11] that knowledge of the actual thickness of the lubricant layer, its rheological properties, and the type of flow is sufficient to predict the behavior of pumping fresh material.

Particle migration is essential for both fluid, and very fluid concretes with a high volume fraction of solid particles. Changes in the rheological properties are serious enough to affect the determination of the flow structure and the injection rate of the pumped concrete [12].

The most important task is to find acceptable rheological properties for applications such as cementing oil and gas wells, where it is necessary to pump cement mortar [13].

The paper [14] presents an experimental study of the influence of the binder type, content, chemical properties of water, and temperature on the rheological properties of the cemented paste material obtained using additives from a copper mine in South Australia.

In order to reduce friction or improve pumpability, in [15] various ultrafine powders are introduced into a high-flow concrete mixture with a low water-binder ratio as a substitute for cement.

The use of a large amount of fly ash in cement-sand solutions significantly increases the fluidity of cement-sand solutions [16].

A set of rheological tests was carried out to assess the torque required for the rotation of steel fibers immersed in various fresh cement pastes and mortar mixtures with the behavior of the Bingham liquid [17]. Fibers with different aspect ratios (length/width) and different geometries, straight and hooked, were rated as the most commonly used. On the other hand, various parameters (the type of mixture, the size of aggregates, the volume fraction of aggregates) that affect the cement mixtures are analyzed, and their influence on the orientation of the fibers is discussed.

Adding superplasticizers to cemented paste can improve its rheological properties and facilitate pumping operations [18].

The properties of shotcrete with different fiber lengths were tested. The proportionality coefficients of the wet shotcrete mixture were analyzed to obtain the optimal proportions of the wet shotcrete mixture [19].

The concrete pumps methods of the distribution of concrete mixtures increase the quality and efficiency of concrete work in the construction of a wide variety of monolithic and prefabricated monolithic structures in industrial, civil, hydraulic, rural, and other types of construction [20,21].

Laying of a concrete mix by concrete pumps includes the acceptance of a concrete transport unit from the concrete mixing equipment into the loading hopper, pumping the mixture through the concrete guide to the place of laying, its distribution in the concreting zone (using flexible hoses or distribution arrows), and related maintenance work for this process [20,21].

Among modern concrete pumps, the most popular are concrete piston pumps with a hydraulic drive that provides smooth operation with reliable performance control, the ability to reverse and feed the mixture through lightweight concrete guides mounted on articulated boom arms with remote control.

Stationary piston concrete pumps are widely used in the construction of high-rise buildings [22,23]. The value of the piston pressure on the concrete is its main characteristic. The piston pressure of the reciprocating concrete pump on the concrete mixture should choose considering the pressure losses in the pipeline during the transportation of the mixture and changes in the performance characteristics of the concrete pump under load. Determining the hydraulic losses in the concrete guide remains relevant at present. Hydraulic losses in the pipeline depending on the specific resistances to the movement of the concrete mixture, the total length of the concrete pipeline, the size of its vertical section, and the local pressure losses in the transition cone bends [20-23]. The work aims to develop an algorithm for selecting a concrete pump that considers the rheological characteristics of the concrete mixture, the hydraulic resistance of the network in the construction of high-rise buildings.

2 Materials and Methods

The main stages of selecting a stationary piston concrete pump using performance diagrams were described in [24, 26]. However, the difference between the actual pump supply and the theoretical one was not taken into account. Previously, it was shown that it is necessary to use the performance characteristics of pumps to select their parameters that correspond to the construction conditions.

The first stage is a preliminary calculation of the pressure drop in the concrete guide at a given feed of the mixture Q . The hydraulic characteristic of the concrete pipeline is the dependence of the pressure drop on the supply of the mixture [20]:

$$P = f_Q = \Delta P + \gamma g H_g, \Delta P = \Delta P_L + \Delta P_M, \quad (1)$$

where ΔP_L , ΔP_M are pressure losses along the length and in local resistances when transporting the mixture through the concrete guide, respectively, Pa; γ is the volume mass of the concrete mixture, kg/m^3 ; g is the acceleration of free fall, m/s^2 ; H is the height of the concrete mixture feed, m.

In order to be able to use the calculation method more widely, including for modified concrete mixes, it is necessary to use a rheological model. Several known rheological models are used to calculate the pressure loss along the length of the pipeline when pumping concrete mixtures.

The Buckingham-Reiner formula (see, for example, [23, 27]):

$$Q = \frac{\pi d^4}{128\mu} \frac{\Delta P_L}{L} \left[1 - \frac{4}{3} \left(\frac{4L\tau_0}{d\Delta P_L} \right) + \frac{1}{3} \left(\frac{4L\tau_0}{d\Delta P_L} \right)^4 \right], \quad (2)$$

where d , L are the diameter and length of the concrete conduit, respectively, m; τ_0 is the ultimate shear stress, Pa; μ is the plastic (structural) viscosity, $Pa \cdot s$.

It was previously established (see [27]) that the calculation of hydraulic losses in the concrete guide by formula (1) gives results more than 3 times higher than the experimental data. It should note that the similar to (2) formula does not have the diameter d in the denominator of fractions in some publications. Also, there is no π multiplier in [23]. The results of calculations based on the Kaplan model are in much better agreement with the experimental data:

$$\Delta P = \frac{4L}{d} \left(\tau_t + \frac{4Q}{\pi d^2} \frac{\eta}{k} \right), \quad (3)$$

$$\Delta P = \frac{4L}{d} \left(\tau_t + \frac{\frac{4Q}{\pi d^2 k} \frac{d\tau_t + d\tau_0}{8\mu + 6\mu}}{1 + \frac{\eta d}{8\mu}} \eta \right), \quad (4)$$

where k is the fill factor, in the first approximation it can be taken to be equal to one.

Formula (3) is intended for the case when the shear stress on the pipe wall is less than the yield strength; otherwise, formula (4) should be used.

For the application of formulas (3), (4), in addition to the previously specified values, it is required to determine with a tribometer the additional parameters τ_t (Pa) and η ($Pa \cdot s/m$) on the surface between the inner cylinder and the concrete mixture. In case of their absence, it is necessary to carry out their estimated calculation. Replace in (3) τ_t by τ_0 , the parameter η is found by the approximate formula $\eta \approx \mu/\delta$, where δ is the thickness of the wall layer:

$$\eta = \frac{\mu}{0,5d - \frac{2\tau_0}{(\Delta P/L)}}. \quad (5)$$

From dependencies (3), (5), it follows

$$Q = \frac{\pi d^2}{4\eta} \left(\frac{d}{2} - \frac{2\tau_0 L}{\Delta P} \right) \left(\frac{\Delta P d}{4L} - \tau_0 \right). \quad (6)$$

From (6) follows the quadratic equation in dimensionless form

$$\Delta p^2 - 2(\theta + 1)\Delta p + 1 = 0, \Delta p = \frac{\Delta P d}{4L\tau_0}, \theta = \frac{4\mu Q}{\pi d^3 \tau_0}. \quad (7)$$

The solution of the quadratic equation (7) allows us to calculate the dimensionless pressure Δp from the relative flow rate Θ :

$$\Delta p = f_1(\theta) = 1 + \theta + \sqrt{(1 + \theta)^2 - 1}. \quad (8)$$

Let us consider some features of the determination of hydraulic pressure losses in local resistances ΔP_M .

In [20], a table is given with experimental data on hydraulic losses depending on the speed of the mixture and the radius of the elbow (rotation by 90°) R . For example, if the speed in a concrete guide with a diameter of $d=100$ mm is 0.5 m/s, then at $R=0,5$ m $\Delta P_k = 39,33$ kPa, and at $R=2$ m $\Delta P_k = 52,47$ kPa. It turns out a paradoxical picture; with an increase in the radius of the knee, hydraulic losses increase. In [28], it was shown that the losses per meter of the arc AB (see 1) decrease with increasing arc radius. But this does not solve the problem, as it does not explain why the absolute losses increase. To explain the resulting paradox, consider the diagram in Fig. 1.

In the experiments in [20], the pressure drop in the pipeline between sections A and B was measured. But the larger the radius of rounding of the elbow, the smaller the pipeline's total length. Reducing the length of the pipeline

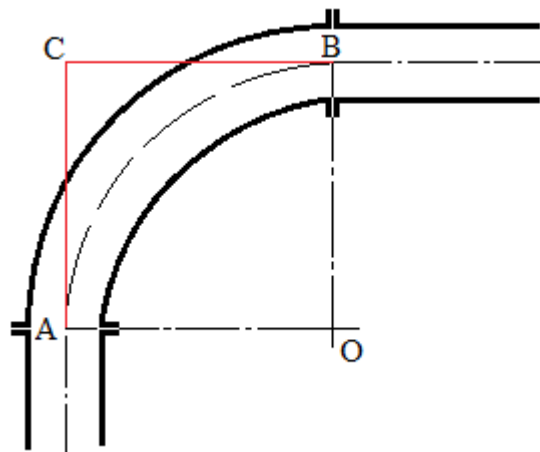
$$\Delta L = |AC| + |CB| - |\overline{AB}| = 2R - 0,5\pi R = 0,43R.$$

The pipeline losses on the length ΔL from the ΔP_k are subtracted to find the hydraulic losses of ΔP_{k0} at the elbow:

$$\Delta P_{k0} = \Delta P_k - \frac{0,43R\Delta P_L}{L}. \quad (9)$$

In the example of the calculation from [20], the specific hydraulic losses along the length of the concrete pipeline $\Delta P_L/L = 24,9$ kPa/m. Then, from the formula (9), for $R=0,5$ m, the $\Delta P_{k0} = 34,0$ kPa is obtained; for $R=2$ m, the $\Delta P_{k0} = 31,0$ kPa. In the latter case, the hydraulic losses are 9,7% less, which corresponds to the physical meaning. But such a decrease can hardly be considered significant, given the low accuracy of the DRC definition. Moreover, this approach does not take into account the rheological properties of the concrete mixture.

Fig. 1. Diagram of the concrete pipeline elbow



Another approach [20] suggests increasing the actual length of the concrete duct L by 9 m for each knee and increasing the estimated length of the transition cone L_C by 3-4 times. The use of the reduced length of the concrete guide L_n in the calculations allows us to take into account the rheological properties of the mixture:

$$L_{\Pi} = L + 9k + 3,5L_C. \quad (10)$$

where k is the number of elbows, L_C is the length of the transition (distribution) cone.

Next, this approach was used to calculate the local hydraulic losses in the concrete guide.

The second stage is to determine the parameters of the piston concrete pump that correspond to the construction conditions. The technical documentation provides diagrams with the pump QT's theoretical performance (flow) (see Figure 2). It is related to the actual flow at a pressure drop P according to the formula:

$$Q = Q_T f_2(P), f_2(P) = 1 - \frac{(1-K)P}{P_H}, K = \frac{Q_H}{Q_T}, \quad (11)$$

where K , Q_H , P_H are the volumetric efficiency, flow, and pressure drop in the nominal mode, respectively.

3 Results and Discussion

Example of the calculation. Let it be required to ensure the supply of concrete mix at least $Q = 45 \text{ m}^3/\text{h} = 0,0125 \text{ m}^3/\text{s}$. The stationary piston concrete pump will be used in the range of height differences and lengths of the concrete pipeline $H_{\min} = 30 \text{ m}$, $H_{\max} = 60 \text{ m}$, $L_{\min} = 90 \text{ m}$, $L_{\max} = 105 \text{ m}$. The inner diameter of the concrete pipe $d = 0,125 \text{ m}$. The number of concrete guide bends $k_{\min} = 6$, $k_{\max} = 11$. The length of the transition cone $L_C = 3 \text{ m}$. Properties of the concrete mixture: $\tau_0 = 28 \text{ Pa}$, $\mu = 50 \text{ Pa} \cdot \text{s}$, $\gamma = 2200 \text{ kg} / \text{m}^3$.

According to the formulas (7), (8) $\Theta = 14,55$; $\Delta p = 31,07$. Then the specific pressure loss

$$\Delta P/L = 4\tau_0 \Delta p/d = 27,84 \text{ kPa}.$$

Hydraulic losses at the highest height and length of the concrete pipeline

$$\Delta P_{\max} = \frac{\Delta P}{L} (L_{\max} + H_{\max} + 9k_{\max} + 3,5L_C) + \gamma g H_{\max} = 8,935 \text{ MPa}.$$

Let the pressure drop value ΔP_{\max} , calculated at the first stage correspond to the nominal pressure (that is, $P/P_H = 1$). The volumetric efficiency (another name is the fill factor) allows you to calculate the theoretical supply of Q_T for a given Q . However, in the manufacturers' technical documentation of reciprocating concrete pumps, there is no information about the efficiency. In [21], the values for the efficiency were obtained experimentally for one of the types of a piston concrete pump with a cone draft of 5-10 cm: $K = 0,75$. Then in the example by the formula (11) $Q_T = Q/K = 16,67 \text{ dm}^3/\text{s}$.

In the working section of the pump performance diagram, the net power N_u , calculated from the theoretical supply, remains unchanged:

$$N_u = P Q_T = \frac{P Q}{f(P)}. \quad (12)$$

The formula (12) gives $\Delta P_{\max} \cdot Q_T = 148,9 \text{ kW}$. Therefore, it is necessary to choose a piston concrete pump in which the N_u parameter has a value of at least the calculated one. Some manufacturers give the value of this parameter directly on the charts. For example, the performance diagram of the Putzmeister BSA 1409-D reciprocating concrete pump [29] shows a value of 140 kW, and the diagram of the JUNJIN JSP.90HP-D reciprocating concrete pump [30] shows a value of 147 kW. In the latter case, after recalculation according to the diagram (Fig. 3), a more accurate value was obtained for the specified pump $N_u = 150,0 \text{ kW}$, which fully satisfies the conditions of the example.

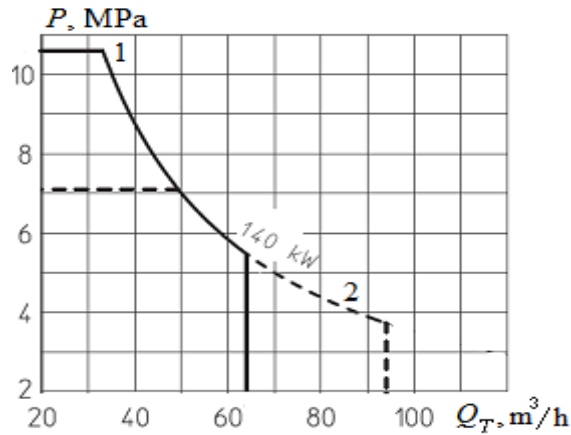


Fig. 2. Performance diagram of a reciprocating concrete pump BSA 1409-D [29]: 1 – piston side, 2 – rod side

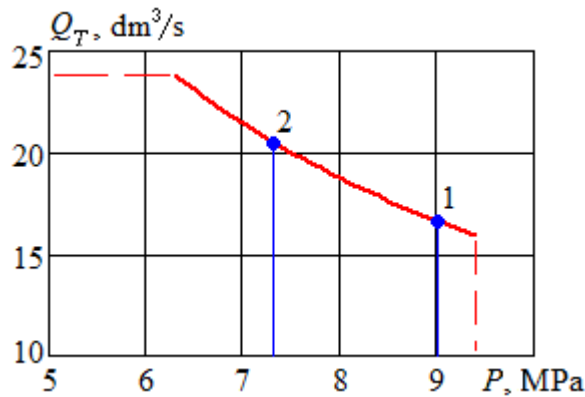


Fig. 3. Performance diagram of the stationary piston concrete pump JSP.90HP-D [30] on the rod side: 1-point corresponds to ΔP_{max} , 2- ΔP_{min}

In the high-flow mode (road side), according to the performance diagram, $P_H = 9.39$ MPa. Higher pressure is not possible, as the safety valve is triggered.

The final stage is the recalculation of the parameters, taking into account the selected piston concrete pump. Characteristics of the concrete pipeline in MPa:

$$F_1(Q_x) = 10^{-6} \left(f_1 \left(\frac{4\mu Q_x}{\pi d^3 \tau_0} \right) \frac{4\tau_0}{d_0} (L_{max} + H_{max} + 9k_{max} + 3,5L_C) + \gamma g H_{max} \right). \tag{13}$$

The solution of equation (13) gives a refined value $Q_{min} = 12,64$ dm^3/s :

$$F_1(Q_x) = \frac{150,0 f_2(F_1(Q_x))}{1000 Q_x}. \tag{14}$$

Similarly, (13), the function $F_2(Q_x)$ is formed at the lowest pressure drop and the supply $Q_{max} = 16.49$ dm^3/s is calculated. Recalculating the differential pressure:

$$\Delta P_{max} = F_1(Q_{min}) = 9,017 \text{ MPa}; \Delta P_{min} = F_2(Q_{max}) = 7,321 \text{ MPa}.$$

Next, the calculation can be performed for the next range of heights.

4 Conclusions

To increase the reliability of the calculation of the actual performance of the piston concrete pump, it is necessary that their manufacturers give the value of the filling factor, at least in the nominal mode.

Currently, it is almost impossible to choose a piston concrete pump according to the energy efficiency criterion, since the technical documentation does not show the dependence of the total pump efficiency (or the power consumed) on the pressure drop.

References

1. Tay, Y.W.D., Qian, Y., Tan, M.J. Printability region for 3D concrete printing using slump and slump flow test. *Composites Part B: Engineering*. 2019. 174. Pp. 106968. DOI:10.1016/j.compositesb.2019.106968.
2. Mohan, M.K., Rahul, A. V., Van Tittelboom, K., De Schutter, G. Rheological and pumping behaviour of 3D printable cementitious materials with varying aggregate content. *Cement and Concrete Research*. 2021. 139. Pp. 106258. DOI:10.1016/j.cemconres.2020.106258.
3. Jones, S.Z. Fused Filament Fabrication Printer Modified to Dispense Cement Paste for Concrete Additive Manufacturing Studies. *Journal of research of the national institute of standards and technology*. 2020. 125. Pp. 125034. DOI:10.6028/jres.125.034. URL: <https://nvlpubs.nist.gov/nistpubs/jres/125/jres.125.034.pdf>.
4. Lu, B., Zhu, W., Weng, Y., Liu, Z., Yang, E.H., Leong, K.F., Tan, M.J., Wong, T.N., Qian, S. Study of MgO-activated slag as a cementless material for sustainable spray-based 3D printing. *Journal of Cleaner Production*. 2020. 258. Pp. 120671. DOI:10.1016/j.jclepro.2020.120671.
5. Chen, Y., Chaves Figueiredo, S., Li, Z., Chang, Z., Jansen, K., Çopuroğlu, O., Schlangen, E. Improving printability of limestone-calcined clay-based cementitious materials by using viscosity-modifying admixture. *Cement and Concrete Research*. 2020. 132. Pp. 106040. DOI:10.1016/j.cemconres.2020.106040.
6. Skripkiunas, G., Karpova, E., Dauksus, M. Rheological behaviour modelling of cement paste with nanotubes and plasticizer. *Journal of Silicate Based and Composite Materials*. 2019. 71(6). Pp. 184–189. DOI:10.14382/epitoanyag-jsbcm.2019.32. URL: https://epitoanyag.org.hu/static/upload/10.14382_epitoanyag-jsbcm.2019.32.pdf (date of application: 9.05.2021).
7. Hosseinpoor, M., Ouro Koura, B.I., Yahia, A. Rheo-morphological investigation of Reynolds dilatancy and its effect on pumpability of self-consolidating concrete. *Cement and Concrete Composites*. 2021. 117. Pp. 103912. DOI:10.1016/j.cemconcomp.2020.103912. URL: <https://www.sciencedirect.com/science/article/pii/S0958946520304169?via%3Dihub> (date of application: 9.05.2021).
8. Jang, K.P., Kim, W.J., Choi, M.S., Kwon, S.H. A new method to estimate rheological properties of lubricating layer for prediction of concrete pumping. *Advances in Concrete Construction*. 2018. 6(5). Pp. 465–483. DOI:10.12989/acc.2018.6.5.465. URL: <http://koreascience.or.kr/article/JAKO201835146898775.page> (date of application: 9.05.2021).
9. Hosseinpoor, M., Ouro Koura, B.I., Yahia, A., Kadri, E.H. Diphasic investigation of the visco-elastoplastic characteristics of highly flowable fine mortars. *Construction and Building Materials*. 2021. 270. Pp. 121425. DOI:10.1016/j.conbuildmat.2020.121425. URL: <https://www.sciencedirect.com/science/article/pii/S0950061820334292?via%3Dihub> (date of application: 10.05.2021).
10. Park, C.K., Jang, K.P., Jeong, J.H., Sohn, Y.S., Kwon, S.H. Analysis on pressure losses in pipe bends based on real-scale concrete pumping tests. *ACI Materials Journal*. 2020. 117(3). Pp. 205–216. DOI:10.14359/51724616. URL: <https://www.concrete.org/publications/internationalconcreteabstractsportal.aspx?m=details&id=51724616> (date of application: 10.05.2021).
11. Secrieru, E., Khodor, J., Schröfl, C., Mechtcherine, V. Formation of lubricating layer and flow type during pumping of cement-based materials. *Construction and Building Materials*. 2018. 178. Pp. 507–517. DOI:10.1016/j.conbuildmat.2018.05.118. URL: <https://www.sciencedirect.com/science/article/pii/S0950061818311851?via%3Dihub> (date of application: 10.05.2021).
12. Fataei, S., Secrieru, E., Mechtcherine, V. Experimental insights into concrete flow-regimes subject to shear-induced particle migration (SIPM) during pumping. *Materials*. 2020. 13(5). Pp. 1233. DOI:10.3390/ma13051233. URL: <https://www.mdpi.com/1996-1944/13/5/1233> (date of application: 10.05.2021).
13. Liu, X., Nair, S.D., Aughenbaugh, K.L., Juenger, M.C.G., van Oort, E. Improving the rheological properties of alkali-activated geopolymers using non-aqueous fluids for well cementing and lost circulation control purposes. *Journal of Petroleum Science and Engineering*. 2020. 195. Pp. 107555. DOI:10.1016/j.petrol.2020.107555. URL:

<https://www.sciencedirect.com/science/article/pii/S0920410520306264?via%3Dihub> (date of application: 10.05.2021).

14. Zhao, Y., Taheri, A., Karakus, M., Chen, Z., Deng, A. Effects of water content, water type and temperature on the rheological behaviour of slag-cement and fly ash-cement paste backfill. *International Journal of Mining Science and Technology*. 2020. 30(3). Pp. 271–278.

DOI:10.1016/j.ijmst.2020.03.003. URL:

<https://www.sciencedirect.com/science/article/pii/S2095268619301971> (date of application: 10.05.2021).

15. Liu, J., Wang, K., Zhang, Q., Lomboy, G.R., Zhang, L., Liu, J. Effects of Ultrafine Powders on the Properties of the Lubrication Layer and Highly Flowable Concrete. *Journal of Materials in Civil Engineering*. 2020. 32(5). Pp. 04020099. DOI:10.1061/(asce)mt.1943-5533.0003193. URL: <https://ascelibrary.org/doi/abs/10.1061/%28ASCE%29MT.1943-5533.0003193> (date of application: 10.05.2021).

16. Balakrishnan, B., Khalid, N.H.A., Ismail, M. Time-dependent rheological behavior of cement-sand injection grout containing high volume fly ash. *IOP Conference Series: Materials Science and Engineering*. 2020. 849(1). Pp. 012033. DOI:10.1088/1757-899X/849/1/012033. URL: <https://iopscience.iop.org/article/10.1088/1757-899X/849/1/012033> (date of application: 10.05.2021).

17. Villar, V.P., Medina, N.F., Alonso, M.M., Diez, S.G., Puertas, F. Assessment of parameters governing the steel fiber alignment in fresh cement-based composites. *Construction and Building Materials*. 2019. 207. Pp. 548–562. DOI:10.1016/j.conbuildmat.2019.02.036. URL: <https://www.sciencedirect.com/science/article/pii/S0950061819303289?via%3Dihub> (date of application: 10.05.2021).

18. Ouattara, D., Mbonimpa, M., Yahia, A., Belem, T. Assessment of rheological parameters of high density cemented paste backfill mixtures incorporating superplasticizers. *Construction and Building Materials*. 2018. 190. Pp. 294–307. DOI:10.1016/j.conbuildmat.2018.09.066. URL: <https://www.sciencedirect.com/science/article/pii/S0950061818322438?via%3Dihub> (date of application: 10.05.2021).

19. Liu, G., Cheng, W., Chen, L. Investigating and optimizing the mix proportion of pumping wet-mix shotcrete with polypropylene fiber. *Construction and Building Materials*. 2017. 150. Pp. 14–23. DOI:10.1016/j.conbuildmat.2017.05.169. URL: <https://www.sciencedirect.com/science/article/pii/S0950061817310681?via%3Dihub> (date of application: 10.05.2021).

20. Zakharchenko, G.A. Ed. Manual for laying concrete mixes with concrete pump installations TSNIIOMTP. 1978. Pp. 1–144. URL: <https://files.stroyinf.ru/Data2/1/4293846/4293846014.htm> (date of application: 10.05.2021).

21. Komarinskiy, M.V. A productivity of reciprocating concrete pump. *Construction of Unique Buildings and Structures*. 2013. 11(6). Pp. 43–49. DOI:10.18720/CUBS.11.6. URL: <https://unistroy.spbstu.ru/article/2013.11.6> (date of application: 10.05.2021).

22. Aldred, J. Burj Khalifa - A new high for high- Performance concretej. *Proceedings of the Institution of Civil Engineers: Civil Engineering*. 2010. 163(2). Pp. 66–73. DOI:10.1680/cien.2010.163.2.66. URL: <https://www.icvirtuallibrary.com/doi/10.1680/cien.2010.163.2.66> (date of application: 10.05.2021).

23. Li, H., Sun, D., Wang, Z., Huang, F., Yi, Z., Yang, Z., Zhang, Y. A review on the pumping behavior of modern concrete. *Journal of Advanced Concrete Technology*. 2020. 18(7). Pp. 352–363. DOI:10.3151/jact.18.352. URL: https://www.jstage.jst.go.jp/article/jact/18/6/18_352/_article (date of application: 10.05.2021).

24. Velikanov, N.L., Naumov, V.A., Koryagin, S.I. Characteristics of Plunger Pumps. *Russian Engineering Research*. 2018. 38(6). Pp. 428–430. DOI:10.3103/S1068798X18060175. URL: <https://link.springer.com/article/10.3103%2FS1068798X18060175> (date of application: 10.05.2021).

25. Naumov, V., Velikanov, N. Consideration of the characteristics of the concrete mix when choosing concrete pump. *IOP Conference Series: Materials Science and Engineering*. 2018. 365(3). Pp. 032017. DOI:10.1088/1757-899X/365/3/032017. URL: <https://iopscience.iop.org/article/10.1088/1757-899X/365/3/032017> (date of application: 10.05.2021).

26. Naumov, V.A., Velikanov, N.L. Simulation of operational characteristics of the water-ring vacuum pumps. *IOP Conference Series: Materials Science and Engineering*. 2019. 537(3). Pp. 032029. DOI:10.1088/1757-899X/537/3/032029. URL: <https://iopscience.iop.org/article/10.1088/1757-899X/537/3/032029> (date of application: 10.05.2021).

Velikanov, N.L.; Naumov, V.A.

Algorithm for Selecting a Concrete Pump in the Construction of High-Rise Buildings;

2021; *Construction of Unique Buildings and Structures*; 95 Article No 9503. doi: 10.4123/CUBS.95.3

27. Le, H.D., Kadri, E.H., Aggoun, S., Vierendeels, J., Troch, P., De Schutter, G. Effect of lubrication layer on velocity profile of concrete in a pumping pipe. *Materials and Structures/Materiaux et Constructions*. 2015. 48(12). Pp. 3991–4003. DOI:10.1617/s11527-014-0458-5. URL: <https://link.springer.com/article/10.1617/s11527-014-0458-5> (date of application: 10.05.2021).
28. Anofriev, P.G., Hrupalov, I.Y., Burov, V.S. Mathematical models of resistance to the movement of concrete mix in the knees of concrete guides. *Construction. Materials science. Mechanical engineering. Ser. Lifting and transport., builder. and expensive. machinery and equipment*. 2014. (79). Pp. 253–260. URL: http://nbuv.gov.ua/UJRN/smmpm_2014_79_29 (date of application: 10.05.2021).
29. Putzmeister Truck-Mounted Concrete Pumps. URL: <https://www.putzmeister.com/web/europe-east> (date of application: 10.05.2021).
30. JUNJIN Heavy Industry Co (South Korea). Concrete pumps. URL: <https://junjin.ir/En/Feature/ShowFeature.aspx?itmlId=51> (date of application: 10.05.2021).